Proceedings Paper:
Forrester, J., Li, L., Yang, Z. et al. (5 more authors) (2022) Performance of Pzt-based piezoelectric transformers for use In high-temperature converters. In: 11th International Conference on Power Electronics, Machines and Drives (PEMD 2022). PEMD 2022 - The 11th International Conference on Power Electronics, Machines and Drives, 21-23 Jun 2022, Newcastle, UK (hybrid conference). IET Digital Library , pp. 41-46. ISBN 9781839537189

https://doi.org/10.1049/icp.2022.1012

PERFORMANCE OF PZT-BASED PIEZOELECTRIC TRANSFORMERS FOR USE IN HIGH-TEMPERATURE CONVERTERS

Jack Forrester[1], Linhao Li[2], Zijiang Yang[1], Jonathan N. Davidson[1], Martin P. Foster[1], David A. Stone[1], Ian M. Reaney[2], Derek C. Sinclair[2]*

[1]*Department of Electronic and Electrical Engineering, University of Sheffield, Sheffield, UK*
[2]*Department of Materials Science and Engineering, University of Sheffield, Sheffield, UK*
**jack.forrester@sheffield.ac.uk*

Keywords: HIGH TEMPERATURE ELECTRONICS, RESONANT CONVERTER, PIEZOELECTRIC TRANSFORMERS

Abstract

Piezoelectric transformers (PTs) are ideally suited for resonant converter applications, owing to their inherent resonant tank circuit, high power density and efficiency. High temperature electronics is an area of research that is increasing in popularity, due to SiC and GaN devices. However, high temperature power electronic conversion is difficult to achieve using traditional passive components due to the novel materials required. In this paper, a PT made from lead zirconate titanate (PZT) is proposed for use in high temperature power conversion.

1. Introduction

Radial-mode piezoelectric transformers (PTs) are an excellent alternative to traditional magnetic transformers for low to medium power resonant converter applications. PTs exhibit an inherent resonant circuit and so require minimal external components to construct a highly dense resonant converter. Additionally, their low EMI and non-flammability make PTs ideal for use in harsh environments, such as high magnetic fields and/or high temperature.

Whilst several piezoelectric materials exist, lead zirconate titanate (PZT) is often used when designing and constructing PTs owing to its excellent properties, which include very high Q factor and high coupling factor. The Curie temperature of PZT materials is typically around 300°C (however, it is dependent on PZT variant) and so they are suitable for use at temperatures up to around 200°C.

There are several potential applications of high temperature converters: for example, oil and geothermal wells for power logging and monitoring tools at temperatures of up to 250°C and 350°C, respectively, and electric and conventional vehicles, powering the motors and sensors at up to 300°C. They are also useful in the aerospace industry for the control circuitry, for motor and breaking controls and simplifying the electrical design, at temperatures of up to 350°C [1], [2].

Whilst researchers have been able to develop individual elements of converters that can operate at high (200°C) temperatures [3], [4], when combining several of these elements together, the resulting converter was only able to achieve about 55% efficiency at 1W and about 65% efficiency at 2W [5]. High temperature materials often used for these components are complex to work with and have several trade-offs compared to traditional materials [6].

In this paper, a PZT PT is proposed as a component for use in high temperature converters. A brief description of the PT is presented, then the PT is analysed at several ambient temperatures up to 200°C. The equivalent circuit components of the PT are extracted and analysed, and then the performance of a PT based converter is examined with the PT heated to several temperatures.

2. Design and construction of PZT PT

A ring-dot PT topology was chosen for this analysis due to its high-power density. Owing to its single disc construction, it does not require adhesives which may degrade the performance of the device at higher temperatures. PZT-85 was chosen as the PZT material owing to its 'hard' piezoelectric properties, which include a large planar coupling factor and a relatively high Curie temperature of 300°C.

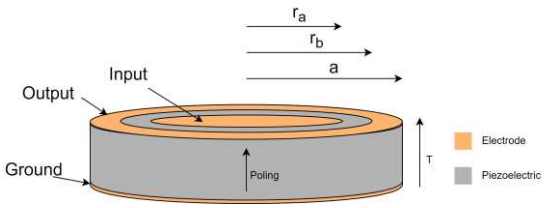

Fig. 1 - Geometry of ring-dot PT

For this application, a PT with radius (a) of 8mm, a thickness (T) of 1.1mm, an r_a = 3.4mm and an r_b = 5.7mm was chosen. The radius and thickness were chosen to achieve a radius/thickness ratio of about 7, ensuring that the PT avoids interaction with spurious modes [7], even though, as Erhart suggests, these modes aren't excited in this PT topology [8]. Secondly, r_a and r_b were chosen to achieve a capacitance ratio ($C_N = C_{in}/N^2C_{out}$) of $< 2/\pi$, to agree with the criterion presented by Foster *et al.* [9], [10]. This ensures that an inductorless half-bridge constructed with this PT will always achieve zero voltage switching (ZVS) irrespective of the load (if the driving conditions presented in [9] are adhered to). The resulting prototype PT is shown in Fig. 2.

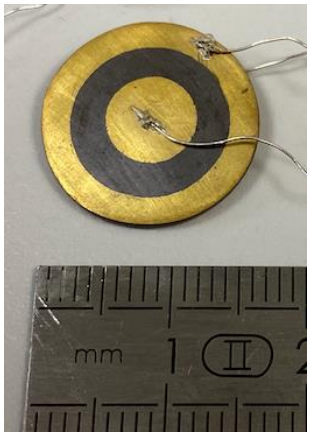

Fig. 2 - PZT PT

3. Testing

The prototype PT was experimentally tested under several ambient temperatures. First, the PT was characterised to determine its small signal equivalent circuit properties and how these properties change with increases in ambient temperature. Second, the PT was used as part of an inductorless half-bridge resonant inverter to evaluate the large signal performance of the PT with changes in ambient temperature.

3.1. Experimental setup

To control the ambient temperature around the PT sample, an Elite tube furnace was used. This furnace allows the ambient temperature to be controlled to a high precision. In order to allow the PT is vibrate freely whilst inside the furnace, the PT was suspended from a ceramic rod, which was clamped into position. This allows the PT to be easily placed inside the oven, as is shown in Fig. 3. The PT was centred within the furnace and cap was placed other the other end of the furnace's tube to aid thermal stability.

Fig. 3 – PT mounted within the furnace

To measure the ambient temperature around the PT accurately, an N-type thermocouple was placed in close proximity (about 1cm away) to the PT within the oven. The temperature from the thermocouple was measured and logged using a Pico TC-08 datalogger connected to a nearby computer. Before each measurement was taken, the temperature was adjusted to the desired temperature, and the transient allowed to settle until no change in temperature was observed for at least 20 minutes.

3.2. Small signal measurements

The small-signal input impedance, Z_{in}, was measured using an Omicron Bode 100 vector network analyser. This is done by shorting the output electrode of the PT to earth, and then measuring the impedance at the input electrode with respect to earth. Similarly, the small signal output impedance, Z_{out}, was measured between the output electrode and earth, with the input electrode shorted to earth. Each impedance measurement was taken at a range of frequencies around the radial resonance. These measurements were then repeated at a range of temperatures, from 25°C up to a maximum of 200°C. For each measurement, the equivalent circuit components shown in the equivalent circuit in Fig. 4 are extracted using the high damping extraction method presented by Forrester *et al.* [11].

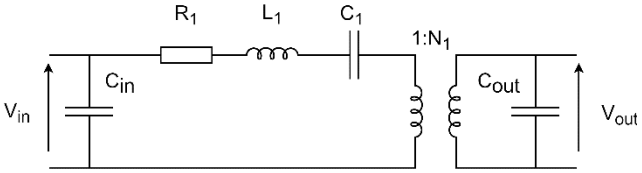

Fig. 4 - Mason equivalent circuit

3.2.1. Damping: Observing Fig. 5, the PT under test exhibits around 15.3 Ω damping at 25°C. The damping then increases with temperature, peaking at 60.7 Ω at 100°C. The damping then decreases with further increases in temperature. Whilst, the lowest damping is achieved at room temperature, only a slight increase in damping is observed at 200°C compared to 25°C. Therefore, we can estimate that the losses exhibited by the PT at 200°C will only be slightly larger than the losses at 25°C.

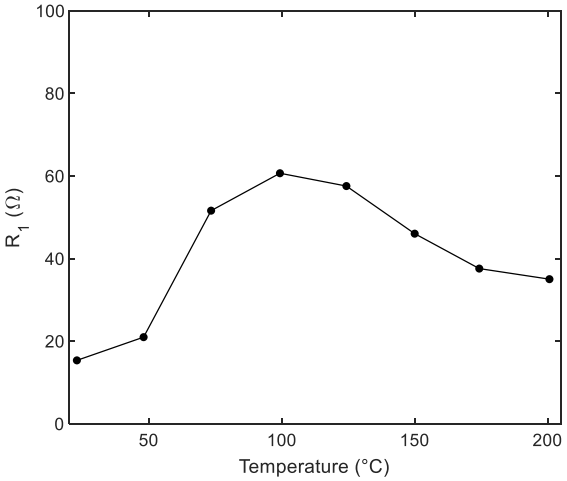

Fig. 5 - Changes in damping resistance against temperature

3.2.2. *Input and output capacitance - C_{in} and C_{out}*: The input and output capacitance exhibited by the PT is shown in Fig. 6.

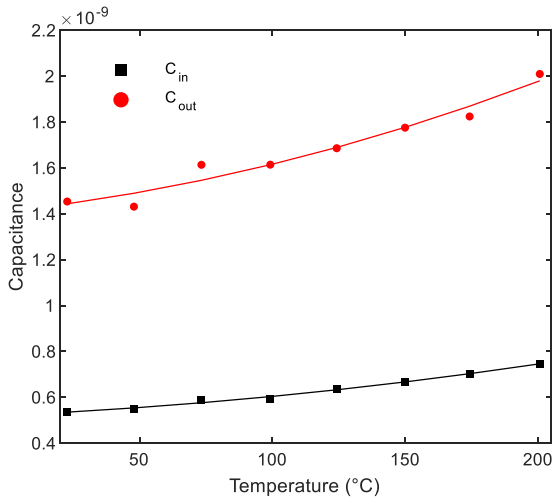

Fig. 6 – Changes in C_{in} and C_{out} against temperature.

In Fig. 6, capacitances C_{in} and C_{out} increase with temperature, as expected, owing to the increase in $\varepsilon_{33}^{\text{T}}$ with temperature as is common in piezoelectric materials. As both sections of the PT are made from the same material, both capacitances change at the same rate with temperature. This also shows that the increased ambient temperature does not cause a noticeable change in the dimensions (shrinking or growing) of the PT such that it causes a change in the electrode area and thus the capacitance. However, an issue that arises with increases in output capacitance, is a reduction in both output power and efficiency, as discussed by Horsley [12]. This may degrade the performance of the converter at higher temperatures.

3.2.3. Resonant frequency: The extracted resonant frequency of the PT is shown in Fig. 7.

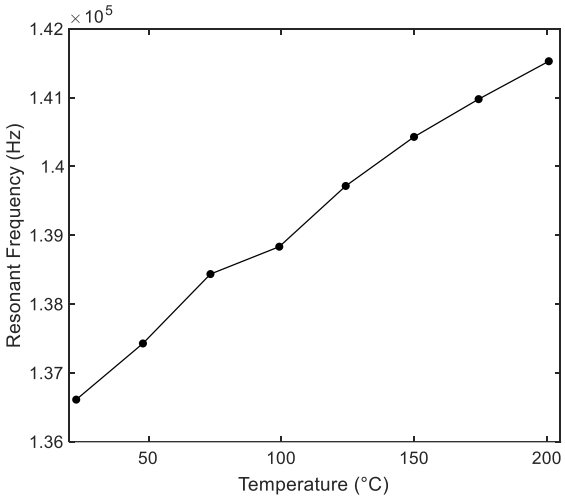

Fig. 7 – Change in resonant frequency against temperature

Observing Fig. 7, the PT's resonant frequency increases approximately linearly with temperature. This change in frequency could potentially cause issues with controlling a PT based power converter, as the frequency of the converter should react to changes in temperature. This is further complicated by the large Q factor of the PT, meaning there is only a small range of frequencies where the converter is operating optimally.

3.3. Large signal measurements

The inductorless half-bridge (Fig. 8) inverter topology was chosen due to its soft-switching ability [13] and to avoid the difficulties associated with high-temperature magnetics. The half-bridge circuit is shown in Fig. 8 with switches S_1 and S_2 forming a half-bridge and with the dashed box highlighting the Mason equivalent circuit for the ring-dot PT.

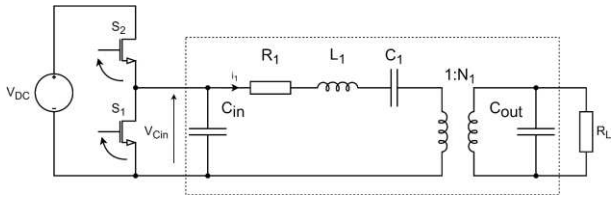

Fig. 8 – Inductor less half bridge inverter, dashed region highlights the Mason equivalent circuit model for the ring-dot PT

The half-bridge-based inverter uses two switches to chop a DC voltage into a high frequency square wave. The MOSFETS are switched in anti-phase, with a deadtime (both switches off) between. The high frequency trapezoidal-like waveform is filtered by the RLC circuit of the PT. Due to the high Q factor of the PT, most (if not all) additional harmonics are heavily attenuated, allowing only the fundamental of the input trapezoidal wave to the PT to pass to the output.

If the PT is designed to the criterion presented by Foster *et al.* [9], zero-voltage switching (ZVS) can be achieved in this circuit, irrespective of load. A full description of the modes of operation during ZVS for this converter can be found in [9], [14].

3.3.1. Method: The power and efficiency of the PZT-based converter was measured across a range of temperatures to evaluate the performance of the converter. During testing, the converter was operated with an 80V DC input, with the half-bridge switches driven in antiphase with a 25% duty cycle. A dedicated ZVS controller based on the frequency doubler phased-locked loop control system described in [14] ensures the converter is operated at resonance by forcing the resonant current to be $\pi/2$ out of phase with the input voltage by controlling the operating frequency.

The input power to the half-bridge and the output power to the load were measured using a Yokogawa PX8000 power scope, allowing the converter efficiency to be calculated. Similarly, the input power to the PT is measured under the same driving conditions, allowing the PT efficiency (i.e. without MOSFET losses) to be calculated and used for further analysis. These measurements were then repeated at

a range of temperatures, from 25°C up to a maximum of 200°C.

To evaluate the performance of the PT fairly, a matched load should be used to compensate for the capacitance variation with temperature. The matched load is calculated using

$$R_{\mathrm{L_{matched}}} = \frac{1}{\omega C_{\mathrm{out}}} \qquad (1)$$

However, as found previously both operating frequency and output capacitance change with temperature. Using (1), the matched load can be calculated for each ambient temperature. The converter exhibits a range of 550-800 Ω for the matched load across the temperature range. To account for this, measurements were taken with a 500 Ω and a 1 kΩ load, and the most efficient measurement taken.

In addition to the experimental converter testing, the converter will be simulated using LTSpice, using the equivalent circuit component values extracted from the characterisation step performed previously. For each temperature step, the input and output power and efficiency will be extracted for comparison to the experimental results.

3.3.2. Output Power and Efficiency:

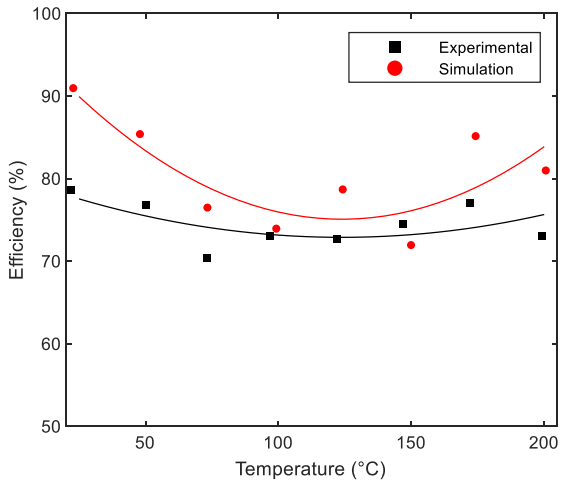

Fig. 9 – Circles show the efficiency of the resonant converter against PT ambient temperature when driving the most efficient load, lines of best fit are also shown

Fig. 9 and Fig. 10 show the output power of the inverter increases with temperature (owing to changes in resonant frequency and the matched load condition), whilst only exhibiting a slight decrease in efficiency comparing the performance at 25°C and 200°C. At 200°C, the converter achieves an output power of around 0.75W with an efficiency of around 75%.

The simulated results show good correlation to the measured results. The efficiency of the simulated converter is higher than the measured results, owing to the simulation model's simplifications (i.e. not including parasitics and additional losses from MOSFETS) but the general trend is similar to the experimental results. The simulated output power matches well with the experimental results, with higher accuracy observed at higher temperatures.

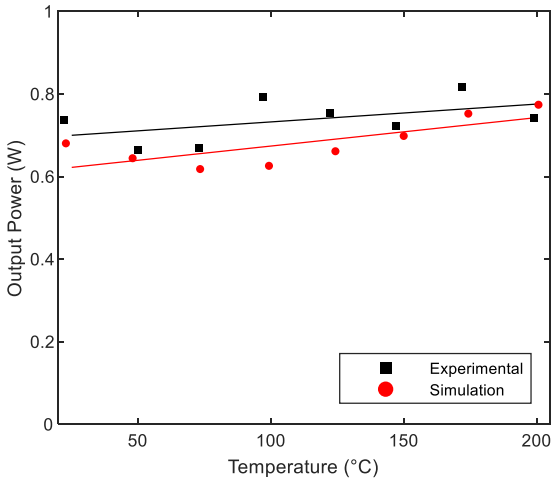

Fig. 10 – Circles show the output power of the resonant converter against PT ambient temperature when driving the most efficient load, lines of best fit are also shown

3.3.3. ZVS: The ZVS ability of the PT can also be evaluated by examining the voltage waveform across the input capacitor; this is shown in Fig. 11.

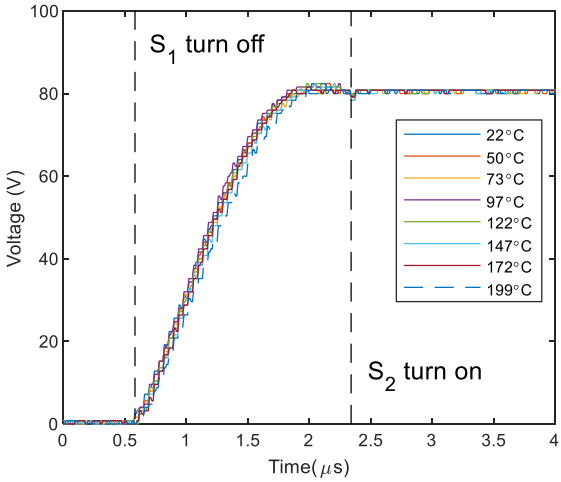

Fig. 11 – $V_{C_{\mathrm{in}}}$ voltage to the PZT PT during the deadtime, with a 500 Ω load at several ambient tempatures

As can be observed in Fig. 11, the converter achieves ZVS (i.e the input capacitor voltage reaches VDC before the end of the deadtime) across the temperature range, this is due to the PT being designed to the critical criterion presented in [9].

3.3.4. Power loss analysis

A breakdown of where power is dissipated (either to the load or as loss) can be generated by comparing the measured converter efficiency to the measured PT efficiency under

the same driving conditions. An area plot of the power breakdown against temperature is shown in Fig. 12.

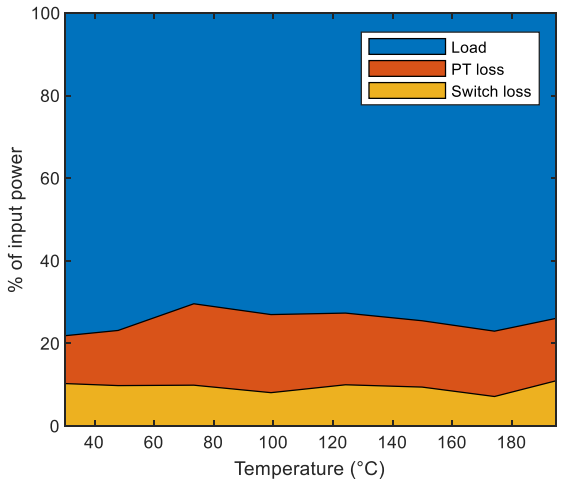

Fig. 12 – Percentage of input power dissipated in the main three elements of the converter, the load, the PT, and the half-bridge MOSFETs

As the converter achieves ZVS across the temperature range then the switching losses in the MOSFETS should be negligible. Additionally, the overall power changes minimally across the temperature range thus the conduction losses should be approximately constant across the range of temperatures. As a result, the loss across the switches stays consistent, accounting for 10% of the input power delivered to the converter. This percentage could be reduced by using MOSFETs with lower $R_{\mathrm{DS_{on}}}$ values, however, $R_{\mathrm{DS_{on}}}$ often comes at the expense of larger C_{DS} capacitances, making ZVS harder to achieve.

Changes in loss in the PT show a similar trend to the changes observed in the damping resistance in Fig. 5, as expected. However, at higher temperatures, the output capacitance increases to approximately 1.5 times its room temperature value and as described in [15], increases in C_{out} also cause the efficiency of the PT to decrease. As a result, the losses in the PT in Fig. 12 stay at a roughly constant for temperatures greater than 100°C, not decreasing as would be expected from the decreases in damping observed at higher temperatures.

4. Discussion

The resulting PT based converter was proven to operate with the PT heated to temperatures of up to 200°C and with minimal degradation in performance. The converter was also able to achieve ZVS across the whole temperature range.

Compared to the results in [5], where the authors were able to achieve an efficiency of ~55% at 200°C with a 1W output power, here the converter achieved ~75% efficiency at 0.75W output power at this temperature. Whilst the output power is lower than that presented in [5], it is likely a similarly high power could be achieved with this PT with a larger input voltage or a smaller load. It can be theorised that, as the PTs efficiency is not affected by the input voltage [15], a 1W output power could also be achieved at a significantly higher efficiency than that in [5].

The PT presented in this paper has a relatively high damping (loss) value compared to similar PTs presented in previous literature [16]. This could be due to the construction of the device or the comparatively low Q factor 200 (vs 1000s) of the material used. If improvements were made to the PT, it is likely that both output power and efficiency could be significantly increased.

In [5], the entire converter was heated whereas this work heats only the PT. However, it is suggested in [17], [18] that both GaN and SiC devices see minimal performance degradation with temperature (even up to 400°C), thus we suggest that a full high temperature PT based converter will achieve similar results to those presented here. GaN and SiC MOSFETSs could also potentially lead to higher efficiencies, as they typically exhibit lower $R_{\mathrm{DS_{on}}}$ values, reducing the conduction loss that was observed to be significant. Additionally, compared to traditional electronics a PT-based approach simplifies a high temperature converter design, as the design and construction of only a single device from common materials is required, compared to designing and constructing several components from novel high temperature materials.

5. Conclusion

The use of PZT PTs in high temperature power converters has been proposed. A sample PT was designed, constructed, and tested under several ambient temperatures. The resulting testing has shown that the performance of a PZT PT degrades minimally even at temperatures of up to 200°C. As a result, a PZT PT based converter was shown to achieve around a 0.75W output power at an efficiency of 75% at 200°C, proving the effectiveness of PT based converters for high temperature applications.

6. References

[1] R. Normann, ‘First High-Temperature Electronics Products Survey 2005’, 2006. doi: 10.2172/889944.

[2] J. Watson and G. Castro, ‘A review of high-temperature electronics technology and applications’, *J Mater Sci: Mater Electron*, vol. 26, no. 12, pp. 9226–9235, Dec. 2015, doi: 10.1007/s10854-015-3459-4.

[3] B. Ray, J. D. Scofield, R. L. Spyker, B. Jordan, and Sei-Hyung Ryu, ‘High temperature operation of a dc-dc power converter utilizing SiC power devices’, in *Twentieth Annual IEEE Applied Power Electronics Conference and Exposition, 2005. APEC 2005.*, Mar. 2005, vol. 1, pp. 315-321, doi: 10.1109/APEC.2005.1452944.

[4] T. Funaki *et al.*, ‘Power Conversion With SiC Devices at Extremely High Ambient Temperatures’, *IEEE Transactions on Power Electronics*, vol. 22, no. 4, pp. 1321–1329, Jul. 2007, doi: 10.1109/TPEL.2007.900561.

[5] R. Perrin, N. Quentin, B. Allard, C. Martin, and M. Ali, 'High-Temperature GaN Active-Clamp Flyback Converter With Resonant Operation Mode', *IEEE Journal of Emerging and Selected Topics in Power Electronics*, vol. 4, no. 3, pp. 1077–1085, Sep. 2016, doi: 10.1109/JESTPE.2016.2544346.

[6] F. Dubois *et al.*, 'A high temperature ultrafast isolated converter to turn-off normally-on SiC JFETs', *IEEE Energy Conversion Congress and Exposition (ECCE)*, Sep. 2012, pp. 3581–3588. doi: 10.1109/ECCE.2012.6342486.

[7] J. Forrester, J. Davidson, and M. Foster, 'Effect of Spurious Resonant Modes on the Operation of Radial Mode Piezoelectric Transformers', in *PCIM Europe 2018; International Exhibition and Conference for Power Electronics, Intelligent Motion, Renewable Energy and Energy Management*, Jun. 2018

[8] J. Erhart, P. Pulpán, R. Dolecek, P. Psota, and V. Lédl, 'Disc Piezoelectric Ceramic Transformers', *IEEE Transactions on Ultrasonics, Ferroelectrics, and Frequency Control*, vol. 60, no. 8, pp. 1612–1618, Aug. 2013, doi: 10.1109/TUFFC.2013.2742.

[9] M. P. Foster, J. N. Davidson, E. L. Horsley, and D. A. Stone, 'Critical Design Criterion for Achieving Zero Voltage Switching in Inductorless Half-Bridge-Driven Piezoelectric-Transformer-Based Power Supplies', *IEEE Transactions on Power Electronics*, vol. 31, no. 7, pp. 5057–5066, Jul. 2016, doi: 10.1109/TPEL.2015.2481706.

[10] S. Ho, 'Modeling of a Disk-Type Piezoelectric Transformer', *IEEE Transactions on Ultrasonics, Ferroelectrics, and Frequency Control*, vol. 54, no. 10, pp. 2110–2119, Oct. 2007, doi: 10.1109/TUFFC.2007.506.

[11] J. Forrester *et al.*, 'Equivalent circuit parameter extraction of low-capacitance high-damping PTs', *Electronics Letters*, Jan. 2020, doi: 10.1049/el.2019.3887.

[12] E. Horsley, 'Modelling and Analysis of Radial Mode Piezoelectric Transformers and Inductor-less Resonant Power Converters', PhD Thesis, University of Sheffield, 2011.

[13] M. Ekhtiari, Z. Zhang, and M. A. E. Andersen, 'State-of-the-art piezoelectric transformer-based switch mode power supplies', in *IECON 2014 - 40th Annual Conference of the IEEE Industrial Electronics Society*, Oct. 2014, pp. 5072–5078. doi: 10.1109/IECON.2014.7049271.

[14] Z. Yang, J. Forrester, J. N. Davidson, M. P. Foster, and D. A. Stone, 'Resonant current estimation and phase-locked loop feedback design for piezoelectric transformer-based power supplies', IEEE Transactions on Power Electronics, pp. 10466 - 10476, 2020, doi: 10.1109/TPEL.2020.2976206.

[15] J. Forrester, J. N. Davidson, M. P. Foster, and D. A. Stone, 'Influence of Spurious Modes on the Efficiency of Piezoelectric Transformers: a Sensitivity Analysis', IEEE Transactions on Power Electronics, pp. 617 - 629, 2020, doi: 10.1109/TPEL.2020.3001486.

[16] S. Priya, S. Ural, H. W. Kim, K. Uchino, and T. Ezaki, 'Multilayered Unipoled Piezoelectric Transformers', *Jpn. J. Appl. Phys.*, vol. 43, no. 6R, Jun. 2004, doi: 10.1143/JJAP.43.3503.

[17] Z. Chen, Y. Yao, D. Boroyevich, K. D. T. Ngo, P. Mattavelli, and K. Rajashekara, 'A 1200-V, 60-A SiC MOSFET Multichip Phase-Leg Module for High-Temperature, High-Frequency Applications', *IEEE Trans. Power Electron.*, vol. 29, no. 5, pp. 2307–2320, May 2014, doi: 10.1109/TPEL.2013.2283245.

[18] T. Nomura, H. Kambayashi, Y. Niiyama, S. Otomo, and S. Yoshida, 'High-temperature enhancement mode operation of n-channel GaN MOSFETs on sapphire substrates', *Solid-State Electronics*, vol. 52, no. 1, pp. 150–155, Jan. 2008, doi: 10.1016/j.sse.2007.07.035.